GSI-FAIR 2025

Report of participation at GSI Helmholtz centre for heavy ion research's summer student program

PREPARED BY :
PITITARAS ATTAPON

According to the royal initiative of Her Royal Highness Princess Maha Chakri Sirindhorn 2025

Introduction

GSI-Fair is a research center located in Darmstadt, Germany. Its main focus is on heavy ion research. From the 21st of July to the 11th of September, Mr. Pititaras Attapon and Ms. Thanaporn Chimruang had the opportunity to attend the summer student program at GSI-Fair. There, I had the opportunity to collaborate in the plasma physics department; therefore, this report book will be focused on the plasma physics department, which is rarely documented in previous report books. Hopefully, I would be able to shed new light on this hidden gem of GSI explored by few students.

The time at GSI did surprise me on all perceptible levels. My expectations before the program were mainly academically oriented, but as time passed by I was surrounded by many activities, opportunities, and lasting relationships ranging from magnificent man-made machines to humble volleyball matches. I truly hope that my experiences at GSI will be able to inspire future generations to explore all the faces of GSI, while helping me to preserve all the good memories there.

Mr. Pititaras Attapon
Science division
Mahidol University International College

Acknowledgment

As a humble physics student, I am grateful to the level beyond describable by languages for this once-in-a-lifetime experience. To work alongside world-leading researchers in a world-renowned institute in such a welcoming environment did not only strengthen my academic knowledge but also shaped my personal perception. Hereby, I would like to humbly thank Her Majesty Maha Chakri Sirindhorn for not only giving me this opportunity but also allowing me to grow into a better version of myself.

This program would not have been possible without all the hard work of the personnel from and related to "The Information Technology Foundation under the Initiative of Her Royal Highness Princess Maha Chakri Sirindhorn." Your hard work did not go unnoticed and is always appreciated by us.

Lastly, I would like to thank all the people related to the GSI summer student program. From all the organizers, researchers, colleagues, and friends, thank you so much for such memorable experiences.

Pititaras Attapon

Table of Contents

1 Facilities & Lectures

1.1 Overview of GSI-Fair

GSI is an accelerator facility in Darmstadt, Germany, focused on heavy-ion research and its applications. It is a unique facility in the world as it can accelerate heavy elements such as uranium. This capability, found in a few places around the world, enables physicists from various disciplines, such as particle physics, nuclear physics, plasma physics, or biophysics, to exploit it and design unique experiments. For this reason, the GSI facility is designed so that accelerated particles can be transported to different departments within the facility.

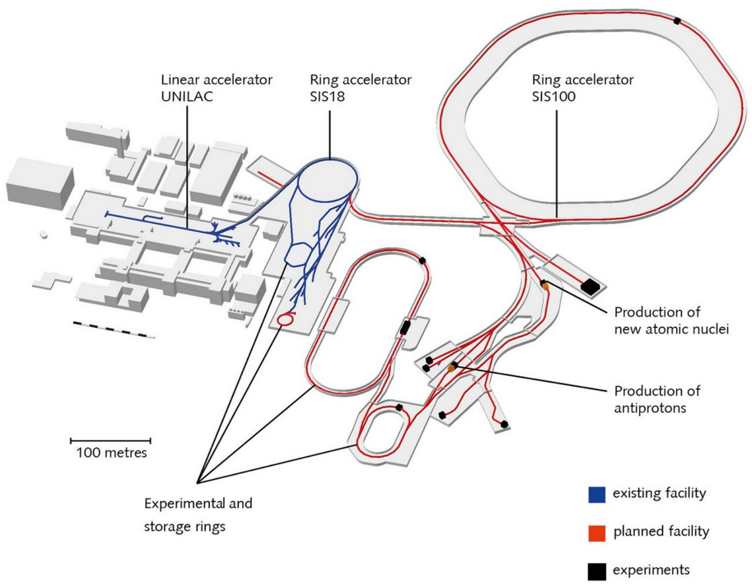

Figure 1: Accelerator network within GSI-FAIR

Experiments at GSI are performed using an accelerator network consisting of many individual parts, as shown in Figure 1 (with the existing facility in GSI colored in blue), allowing many simultaneous experiments.

To accelerate a particle beam, a gas of the target element is injected into the “ionization chamber” with the duty to split the electrons away from the atom. As the nuclei are now naked and positively charged, they are sent into the Universal Linear Accelerator (UNILAC), shown in Figure 2, for acceleration by electric fields. Magnets at the end of the UNILAC adjust the path of ion beams. Here, the beam can be directly sent into the main experimental hall for experiments or to the synchrotron (SIS18) for further acceleration. Some other apparatus found in the network are storage rings and a fragment separator serving different purposes. The storage rings, i.e. ESR and

CRYRING, are used to store particle beams and cool down the beam, reducing the velocity distribution of the particles, allowing more precise experiments, while the fragment separator selects ions by the particle's charge to mass ratio according to the requirements of different experiments.

Figure 2: UNILAC accelerator

To extend the range of experiments possible at GSI, a new connected facility called FAIR is under construction. Fair, shown in red in Figure 1, is equipped with a larger synchrotron to increase the energy of the accelerated particles. This new facility will allow researchers to replicate conditions found within a giant supernova, or even generate antimatter.

1.2 Materials Research Lecture

Material research is a part of the APPA research field in the GSI-Fair. The APPA consists of "Atomic Physics and Fundamental Symmetries", "Plasma Physics", "Radiation Biology and Tumor Therapy", and "Materials Research." The main research fields conducted in this department may be separated into four main sections as follows: Radiation hardness from bulk to nano, Ion-track nanotechnology, Materials under extreme conditions, and User facility + irradiation service.

The lecture by Frieder Kock from the Materials Research Department mainly focused on ion-track nanotechnology. He explained the interaction between material and projectile ions of different energies. The effect can be separated into two parts, i.e. surface and bulk. He further explained the different applications of research conducted in the department. For example, the ions can be used to penetrate irradiated living cells to study their repair processes or to create materials containing nano-sized channels formed by projectile particles.

1.3 Compressed Nuclear Matter Lecture

The lecture on Compressed Nuclear Matter was split into several parts, but it mainly focused on the fundamentals of the Standard Model and Quantum Chromodynamics (QCD). The lecture by Christian Sturm began with basic definitions in the field, such as the use of electron Volts (eV) as an energy unit. The lecture then discussed the strong nuclear force model that governs QCD. He discussed how a portion of an atom's mass is generated by the strong nuclear force, not by the traditional mass of particles we are used to.

The phase diagram of strongly interacting matter was then discussed. Many lecturers occasionally presented this phase diagram during our stay at GSI. It shows how ordinary Hadrons and atomic nuclei can undergo a phase transition to the Quark-Gluon plasma—a plasma of free quarks and gluons that continuously generate new particles due to the strong nuclear force within. The lecture then explained how experiments such as the Compressed Baryonic Matter (CBM) experiment can be conducted to study such an extreme state in the universe.

1.4 Experimental Hadron Spectroscopy Lecture

This lecture presents the definition of Hadrons. A significant amount of time was spent establishing the understanding and definition of Hadrons. In short, Hadrons are bound states of quarks and gluons, as if gluons are gluing together the quarks. We were then taught how to distinguish between different types of Hadrons and quarks.

The lecture then went on to other topics, such as QED and QCD, but one of the most interesting parts was the discussion of Exotic Hadrons. As its name suggests, exotic hadrons are unconventional types of hadrons that are unusually observed. Some configurations of these hadrons are Hybrids, Glueballs, Multiquarks, or even Molecules. The new FAIR (Facility for Antiproton and

Ion Research Figure 3) facility will focus on exotic hadrons. A multi-purpose detector system called PANDA in FAIR is specifically designed for this purpose.

Figure 3: FAIR construction site

1.5 Biophysics Lecture

Currently, cancer is known to be one of the most dangerous diseases, which is very hard to eliminate; however, the biophysics department at GSI is performing techniques offering high precision elimination of cancer in hard-to-reach areas such as the brain. This lecture began with a review of basic radiation knowledge. We were taught how radiation damages our DNA and the amount we can receive without causing harm.

The importance of research on energetic heavy ions was emphasized to us, as space is filled with highly energetic particles. Hence, their effects on astronauts must be studied. However, that is not all; knowledge of the interaction between living cells and highly energetic particles can be brought down to Earth to treat cancer with precision and minimal background damage. By using accelerated ions from particle accelerators, they can be targeted to specific areas of the body containing tumor cells. The Bragg-peak characteristics of the energy release from these ions enable precise targeting of tumor cells, while leaving other areas of the body minimally affected. As the particles are incredibly tiny, patients undergoing this process would not feel any pain.

1.6 Atomic physics Lecture

One focus of this lecture was the storage and cooling of ions in ESR, CRYRING, and HITRAP machines. Instead of shooting ions into targets and having to repeat the experiments many times, a storage ring such as ESR, CRYRING, or HITRAP can be used to store high-energy ions in an orbit and perform measurements each time they pass by. Ions from accelerators are injected into the storage rings, where electromagnetic fields within the storage rings are used to control the path of ions. The magnets used in the storage rings are a combination of dipole, quadrupole, and hexapole magnets. The arrangement of these magnetic fields ensures that the ion bunches are grouped and do not deviate outside the storage ring, where they could hit the storage ring wall.

Another device installed within storage rings is an electron cooler that cools ions. In this sense, cooling of ions does not refer to reducing their temperature but narrowing down their velocity distribution. This device is essential for controlling velocity and its spread within ion bunches, ensuring reliable control error bars for further analysis. This device functions by shooting electrons into the storage rings alongside the ions. An electric field generated between ions and electrons is used to slow the spread of velocity within the ion bunch.

1.7 Nuclear Structure and Astrophysics Lecture

The lectures on Nuclear Structure and Astrophysics are split into three parts. The first one discusses nuclear structure and how to probe its internal structure. The second one discusses the methods and tools used for research, while the third one discusses experiments performed at the ESR (Figure 4).

The main idea from the first lecture was the structure of the nucleus and its models, such as the shell model and Nucleosynthesis. It was here that the experiment NUSTAR was introduced. This experiment aims to simulate neutron star collisions inside the FAIR laboratory. In this lecture, methods for studying the interior of the nucleus were discussed. One method may be to smash them apart and see their reactions. The second lecture then delved deeper into the NUSTAR experiment, focusing on its design principles and structure.

The third lecture then discusses some quantities that can be retrieved from the ESR storage ring. It started with the concepts of storage rings and electron cooling, similar to the atomic physics lecture. This lecture then delved deeper into spectrometry performed within the storage ring, using the Fourier transform to distinguish different ion species. Using the methods mentioned along with careful experimental design, the team at ESR claimed to be the first in the world to detect the Two-Photon Decay, showing unique possibilities for nuclear and astrophysics at GSI.

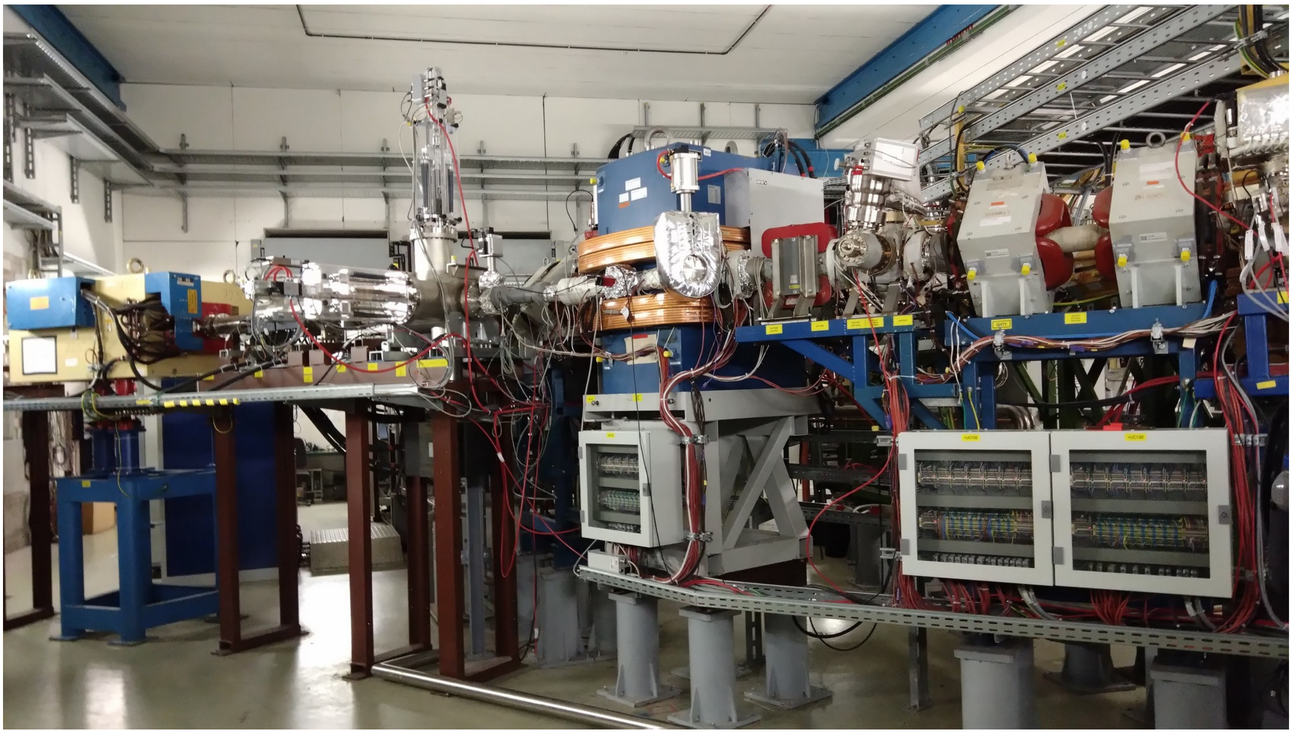

Figure 4: Ion injection point into ESR

1.8 Computing for physics experiments Lecture

Taking a different approach from other theoretical and experimental physics, this lecture on computing for physics experiments offers another rarely discussed aspect of physics. This talk highlights the unique role of computing in physics, design, and infrastructure.

The uniqueness of computation in physics occurs from the tremendous amount of data acquired from experiments and the time constraints of a few milliseconds. Not only this, computation in physics must also deal with different types of data commonly found in other computational fields, as well as coupling between Hardware and Software. With all these requirements, computation in physics becomes the intersection of cutting-edge science, extreme engineering, and high-performance computing.

Simulation is an essential tool for optimization. It can be used to analyze the data for testing, efficiency testing, corrections, or background studies. This step is divided into two parts: Event Generators and Detector Simulation. The data volume in experiments may reach 100 TB per second. This extremely high volume requires a well-designed pipeline and a trigger to remove unusable data. Once the raw data is acquired, another important step is to reconstruct its meaning.

An example of this process is reconstructing particle trajectories within a detector. To meet these requirements, a data center within GSI called Green Cube has been established to perform high-demand computations while remaining environmentally friendly. The following figure shows a set of computers in Green Cube.

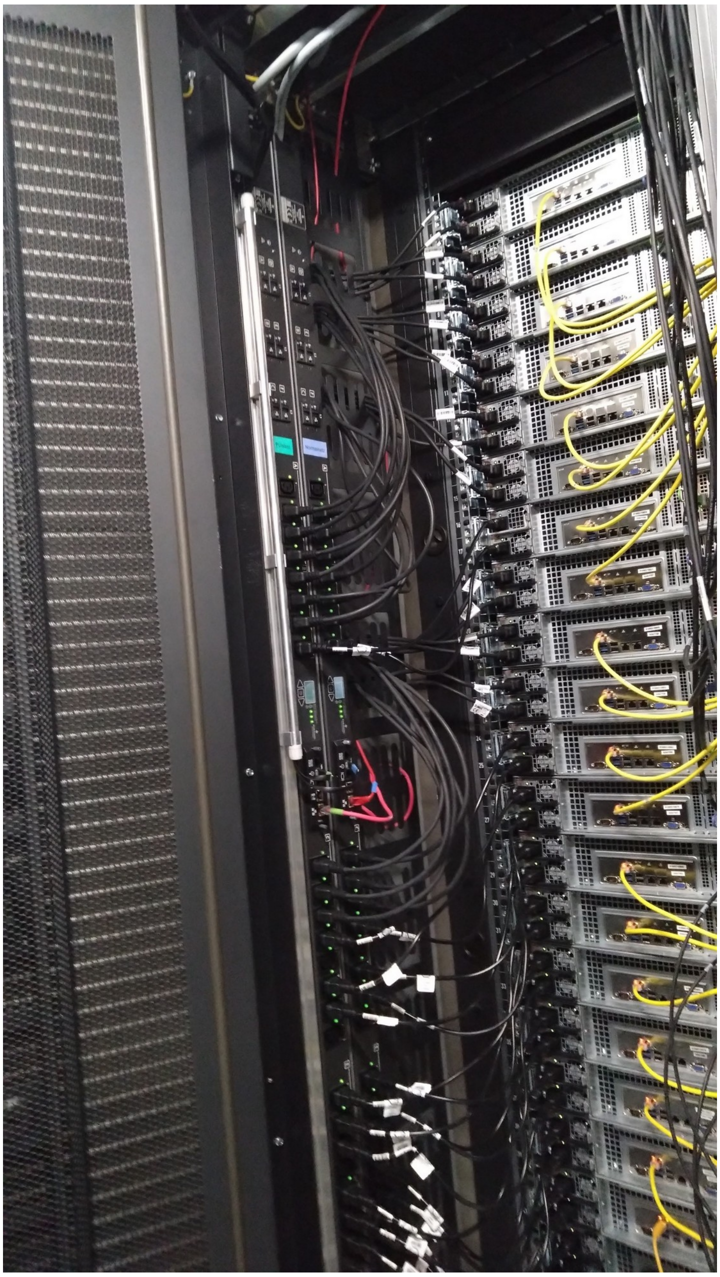

Figure 5: rack of computer array in Green Cube

2 Plasma Physics department

Although plasma physics accounts for only approximately 5% of GSI, it is a unique space for research because globally it is the only facility where usage of particle accelerators and plasma generated by high-energy lasers can be combined. The plasma physics department is a special department at GSI because of its high-energy lasers, PHELIX and NHELIX, used to generate plasma. With the lasers, the plasma physics department can perform its own experiments, with or without accelerators. Hence, in times when accelerator time slots are full, plasma physics research can still be conducted. Still, the combination of accelerators and lasers provides experimental opportunities unavailable anywhere else. For example, ions can be generated by the UNILAC accelerator and sent through laser-generated plasma to simulate the conditions of ions traversing cosmic plasma, such as nebulae.

2.1 Nuclear Fusion

Another primary focus of the plasma physics department at GSI is fundamental research in nuclear fusion. Nuclear fusion is a process that is most commonly observed at the core of stars. The core of stars consists of highly energetic nuclei freely moving within a plasma. The kinetic energy of the nucleons is so high that they can overcome the Coulomb barrier, allowing the strong nuclear force to bind the nuclei together and form heavier elements. This interaction is known as nuclear fusion.

For decades, it has been a dream to replicate nuclear fusion reactions on Earth and harness the energy they produce for clean energy. To generate such a reaction on Earth would be equivalent to creating the sun. Currently, nuclear fusion is the primary focus of many research institutes worldwide, including ITER in France, MAST in the UK, NIF in the USA, LHC in Japan, and TT-1 in Thailand. The Thailand Institute of Nuclear Technology (TINT) houses the only nuclear fusion research machine in ASEAN. There, hydrogen gas is pumped into a device called a tokamak. Ohmic heating is applied to the gas to generate plasma. Magnetic fields generated by coils surrounding the device levitate the plasma, confining it within the machine. This technique of plasma generation and confinement is called magnetic confinement fusion and is also used at the leading nuclear fusion research institute, ITER. However, at GSI, another method, inertial confinement (ICF), is used to generate plasma.

Instead of confining plasma for an extended period within a machine, inertial confinement fusion uses a high-energy laser to irradiate target pellets of deuterium and tritium, generating plasma and enabling nuclear fusion. In 2022, this nuclear fusion technique was the first to release more energy than it consumed, and for the first time demonstrated nuclear fusion's capability as an energy source.

2.2 Laser facility in GSI

As a laser is a crucial part of ICF, a large portion of personnel and effort in the plasma physics department is devoted to the laser. Petawatt High-Energy Laser for Heavy Ion Experiments (PHELIX) and Nanosecond High-Energy Laser for Heavy Ion Experiments (NHELIX) are privileged to the plasma physics department. PHELIX laser can operate in long pulse (1-10ns) and short pulse (0.5-20ps) with maximum energy of 1kJ for the long pulse and 140J for the short pulse. It is also longer than the NHELIX laser, which can only operate in the long-pulse mode (7 ns) with a maximum energy of 120J.

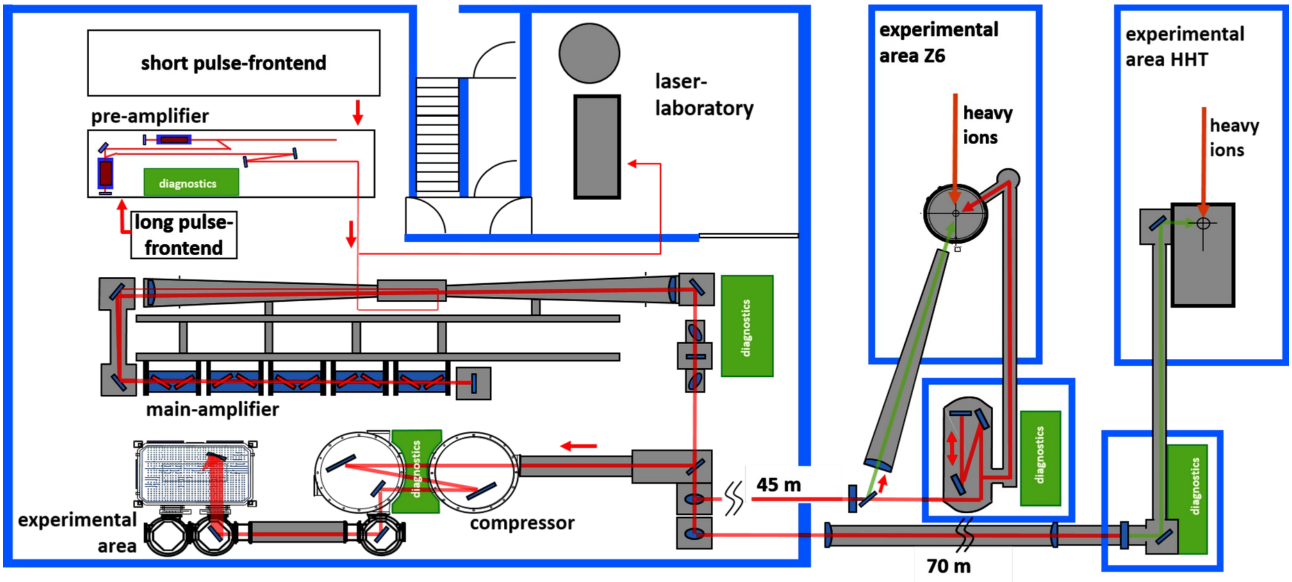

Figure 6: Diagram of PHELIX laser generation and transport

To understand the generation of such high-energy lasers in GSI, the process of laser generation must be explored. Figure 6 shows the process of PHELIX laser generation at GSI, including transport. At the start of laser production (frontend), the laser itself is a harmless small laser. The laser is sent to a preamplifier to amplify it for the first time. The laser is transported into the preamplifier until an energy threshold is reached. The laser is then sent toward the main amplifier; however, because it now has sufficient energy to damage optical instruments during transport, it is elongated to reduce its intensity.

The main amplifier of the PHELIX laser contains layers of crystal structures oriented to form a Brewster angle with the incoming laser. As the laser enters the main amplifier, the power supply on the upper floor of the building dumps all the energy it has been storing over the past hours, generating an intense flash of light within the main amplifier. Energy from this intense light flash is stored in the crystal structure and picked up by the laser as it passes through. At the end of the main amplifier is a mirror adjusted so that a slight angle of degrees is formed between the incoming laser ray and the mirror's normal vector. This way, the laser's path is slightly adjusted from its incoming path. The laser then moves through the main amplifier again, harvesting the remaining energy.

As the laser path is now slightly deviated from its incoming path by the mirror, it does not reverse toward the frontend. Instead, it follows another designated path to the experimental hall. Here, the path for the laser can be chosen to the experimental chamber to which the laser should be transported. Before the experiment is performed, the laser undergoes one final step of compression to counteract the elongation introduced earlier. This compression technique allows the laser's maximum energy to strike a target simultaneously and generate plasma.

As a consequence of laser amplification, the laser's diameter increases with its energy. A tube used to transport the PHELIX laser to the experimental hall has a diameter of about 30 cm. The working principle of the NHELIX laser is similar, but without crystal amplification. A transport pipe for the NHELIX laser can be seen in Figure 7.

Figure 7: Transport pipe for NHELIX laser

2.3 Plasma physics experimental Hall and other facilities

There are three experimental halls for plasma physics, each with its own designated area of study. The first experimental hall is located in the same building as the PHELIX laser, as shown in the bottom left corner Figure 6. This experimental area is not connected to any accelerators; hence, it is used for experiments that require only lasers. The second experimental hall is located in the main experimental hall at GSI, at the end of the UNILAC accelerator. Z6 experimental area, where I worked, and HHT are located in this experimental hall, along with other experimental areas from other departments. Here, experiments combining lasers and UNILAC accelerators can be done. Figure 8 shows the entrance and target chamber of Z6. During experiments, ions and lasers will go into this vacuum chamber. Toward the end of the summer school, construction in the main experimental hall required everyone working there, including me, to wear a safety helmet, a safety vest, and safety shoes. The construction noise was occasionally loud, so I had to use the hearing protection device in the lab.

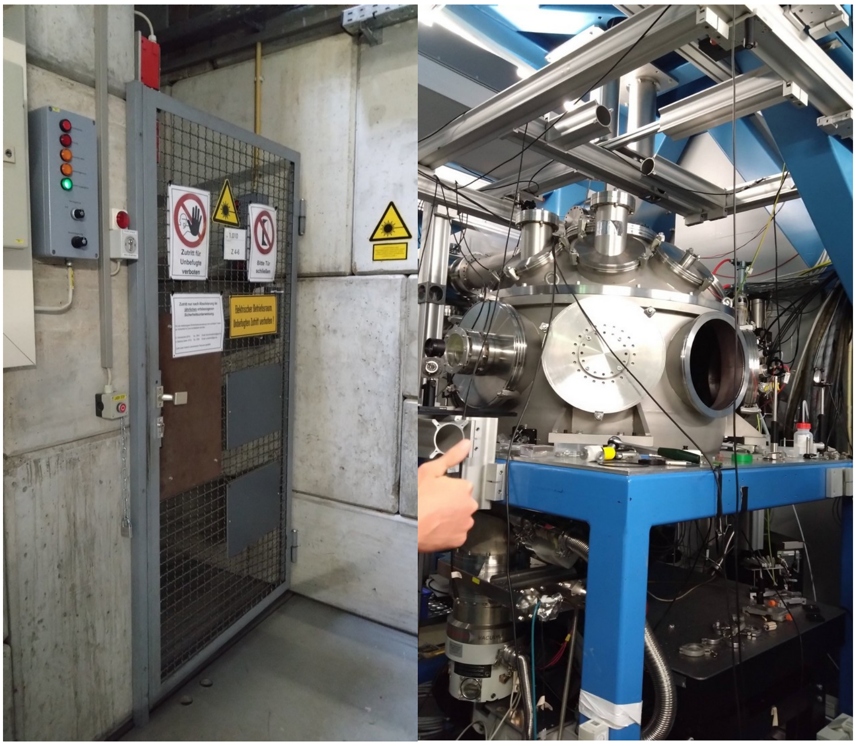

Figure 8: Entrance and target chamber of Z6 experimental area

The last experimental hall of plasma physics is connected to SIS18, which yields ions with higher energy. One example of an experiment conducted in this hall is the study of the effects of ions and plasma on matter.

Figure 9: Building and shared office of plasma physics department

In addition to the experimental halls, the plasma physics department also has its own office. Most of the personnel stay in the C12 office next to the main experimental hall. Images of the plasma physics department and my shared office are shown in Figure 9. Different control rooms are scattered throughout many buildings, including next to the Z6 and PHELIX buildings.

3 Summer School Research at GSI

3.1 Ion stopping power experiment

To understand the motivation behind my research project at GSI, a broader context for ion-stopping-power research in plasma within the department must first be established. Ion stopping power is the energy loss of ions as they travel through matter, or, in this case, plasma; it is defined as (-dE/dx). Although the understanding of ion stopping power in cold matter is clear, the same could not be said for plasma. Different models based on different axioms - such as the standard perturbative model, TM, and BPS - have been developed to explain the ion stopping power in plasma; however, significant contradictions in prediction occur in the scenario where the velocity of the incoming projectile (v_p) is approximately equal to the plasma's electron velocity (v_e).

Determining the correct model of ion stopping power is a primary objective in the plasma physics department. In 2017, W. Cayzac, along with the plasma physics and other personnel in GSI, published the paper "Experimental discrimination of ion stopping models near the Bragg peak in highly ionized matter." The experiment reported in this paper used the UNILAC to accelerate carbon ion beams through laser-generated plasma in an attempt to discriminate among the many models of ion stopping power in plasma. Because stopping-power models must be discriminating in the region where v_p/v_e is close to 1, the energy of ions emerging from the UNILAC accelerator at 4 MeV/u is too high and must be reduced using a degrader to approximately 0.5 MeV/u. This experiment allowed rejection of standard perturbative models while supporting the TM and BPS models. However, it was later realized that the use of accelerated ions from the UNILAC and a degrader contributed to a loss of precision in distinguishing closely related models of TM and BPS.

A new experiment, an improvement on W. Cayzac's 2017 results, is planned for the upcoming year by the LIGHT beamline collaboration, consisting of research institutes and universities in Germany. Using new ion-generation techniques, this experiment will allow further discrimination of the remaining models. Instead of using high-energy ions generated by the UNILAC accelerator, the new technique will accelerate ions using lasers via the TNSA mechanism (Figure 10). In a nutshell, the TNSA mechanism is a process in which a high-energy laser is fired at a thin target foil, e.g., a pure carbon foil, imparting electrons in the impacted region with forward momentum to the other side of the target foil. As electrons accumulate on the side toward the plasma target, an electric field is generated between the target surface and the electron-accumulated region. When a laser impacts a target and generates an intense electric field, the released particles are guided toward the target, allowing the acceleration of particles that require only the length of a thin target rather than meters-long accelerators.

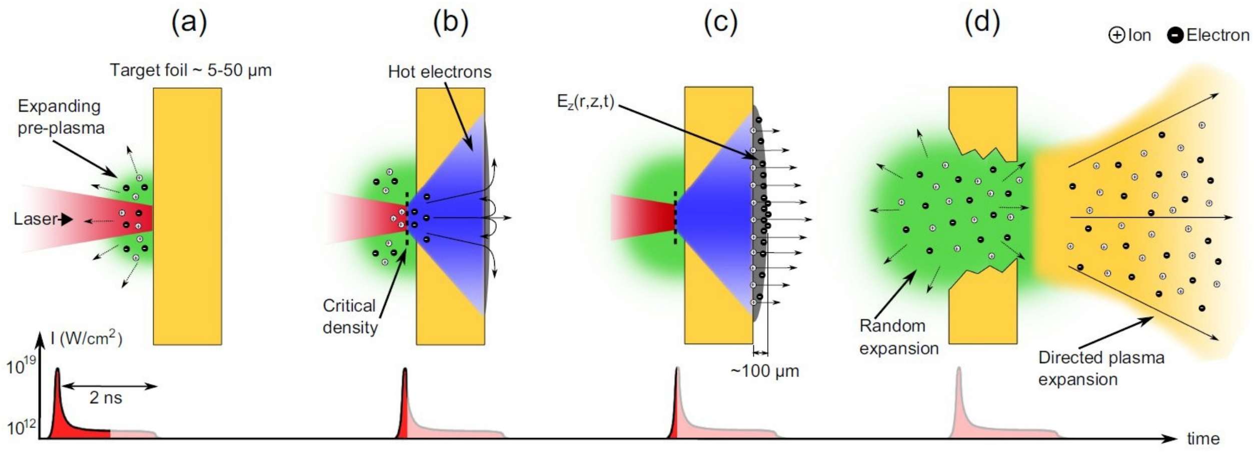

Figure 10: Ion Generation: the TNSA mechanism

Ion stopping power is not a quantity that can be directly measured; hence, it is measured through the energy loss of ions traveling through plasma. The simplified schematic of the planned ion-stopping-power experiment is shown in Figure 11.

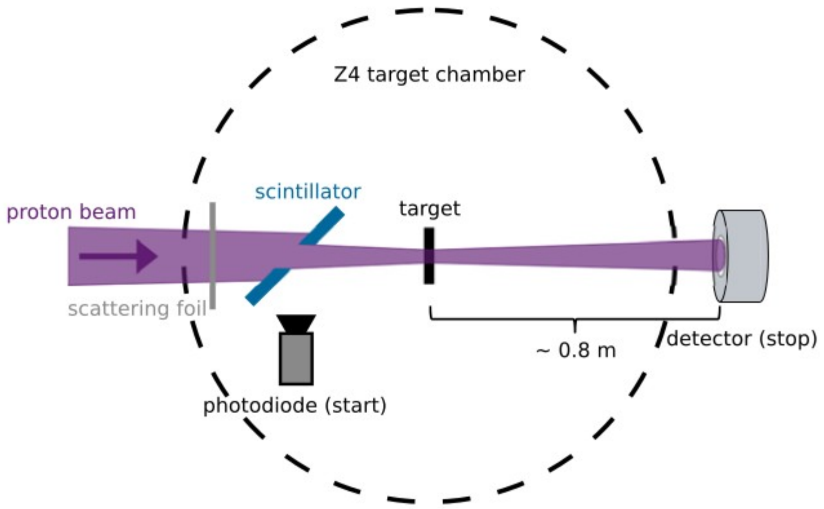

Figure 11: Simplified schematic of ion stopping power experiment

In this figure, the ions generated using the TNSA mechanism are transported into the target chamber. The ion beam with a known velocity first passes through a pinhole to ensure its trajectory. Then, the ion beam passes through a scintillator, emitting gamma radiation detected by a photodiode. As the photodiode detects the gamma radiation, it establishes the start time (t_0). Next, the ion beam passes through a plasma target generated by lasers and is directed toward the stopping detector. The stopping detector records the time of arrival of the ions (t_f). With the distance between the plasma target and the stopping detector known. The Time of Flight (TOF) can be calculated using the following formula:

$$TOF = (t_f - t_0) – (v_0 \text{ x } L_0).$$

In this equation, v_0 and L_0 correspond to the velocity of the ion beam before encountering the plasma and the distance between the scintillator, respectively. With the time of flight known, the velocity of the ion beam after encountering the plasma can be determined with

$$v_f = L_{TOF} / TOF.$$

Here, L_{TOF} is the known distance between the plasma target and the stopping detector. Once the velocity of the ion beam after traveling through plasma is known, its kinetic energy can be calculated. With the final kinetic energy known, the energy loss of the ion before and after encountering the plasma can be calculated. To relate the measured energy loss to ion stopping power in plasma, the integral of the stopping power with respect to the path taken by each ion in a Monte Carlo simulation is computed. This way, the measured energy loss can be compared with each model of ion stopping power.

The stopping detector used in this experiment is a CVD diamond detector, which is my research topic at GSI. My goal was to characterize a CVD diamond as a preparation for the ion-stopping-power experiment.

3.2 Summary of summer research at GSI

Each participant in the GSI summer school program must submit a 4-page report to GSI detailing their research at GSI. All reports from each participant, along with funny reports and pictures taken during the program, are compiled into a single book and distributed to each student. Two books are given to each participant. Typically, the students will give one of the books to their tutors and keep one for themselves. In our year, we all signed each other's books as a piece of memory.

As the reports are publicly available online, my report submitted to GSI is included in the appendix. Due to the length constraint of the reports, the following sections cover the main details of the experiment and those not covered in the report submitted to GSI.

Research experience at GSI

Topic: Characterization of CVD diamond detector

Author: Pititaras Attapon

Objective:

A new test design for a CVD diamond detector with four distinct sections is developed to determine the optimal electrode configuration for the ion-stopping power experiment. The characteristics of each quadrant are unknown; hence, each quadrant must be characterized. The characterization of three characteristics in each quadrant is planned, namely: efficiency with respect to bias voltage, response function, and efficiency at low ion energy. Here, efficiency refers to the detector's ability to detect ions under different setups. The goal of this project is to determine the electrode design that is most suitable for low-energy ions.

Background and Importance:

The CVD diamond detector will serve as the stopping detector, an essential component of the planned ion-stopping-power experiment using the TNSA ion acceleration technique. From the low energy requirement of the ion stopping power experiment, where the velocity of the incoming ion is approximately equal to the plasma's electron velocity, the diamond detector must be capable of detecting ions with energy less than 500 keV/u. Hence, efficient detection of charges at low energy is a crucial part of the ion-stopping-power experiment.

Theory and working principles

The standard model of a diamond detector consists of a thin diamond film "sandwiched" between a pair of positive and negative electrodes, as shown in Figure 12. The working principle of the CVD diamond detector is relatively simple. As an ion travels through the diamond, it will lose energy to atoms within the diamond film. The increase in the energy of atoms in the diamond film leads to ionization, creating an electron-hole pair. Due to the presence of an electric field between the two electrodes, the electron with a negative charge will be attracted toward the positive electrode. In contrast, the hole with a positive charge is attracted toward the negative electrode. The arrival of an electron and its corresponding hole at the electrodes corresponds to an electrical current from the detector, which can be read with an oscilloscope.

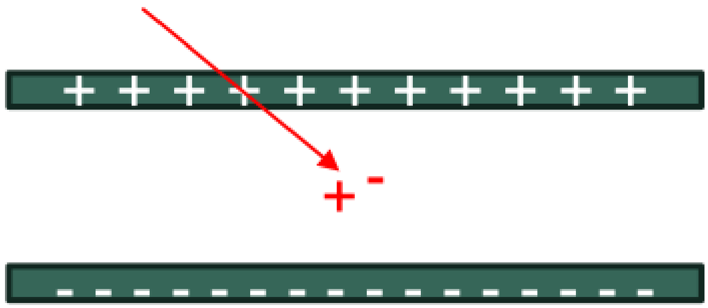

Figure 12: Schematic of standard CVD diamond detector

Still, the standard diamond detector model performs poorly for low-energy ions. Low-energy ions lack the energy to reach the center of the diamond film. Instead, they will stop near the surface, increasing the probability of electron-hole recombination. To overcome this problem, a new design of CVD diamond detector (Figure 13) is proposed. In this new design, the electrodes are moved to nodes on the detector surface rather than sandwiching the diamond film. Relocating the electrodes to the top of the detector yields a stronger electric field near the surface; hence, a better expectancy of charge collection efficiency near the surface. The improvement of this design is also the cause of its drawback in detecting moderate- or high-energy ions, as electron-hole pairs created farther from the diamond surface are more likely to recombine.

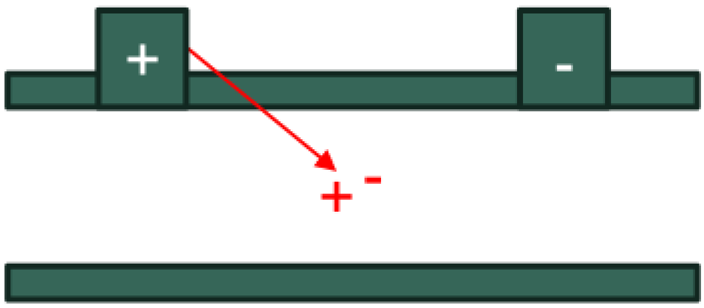

Figure 13: Schematic of CVD diamond detector for low energy ion

An image of the diamond detector to be characterized in this research project is shown in Figure 14. This diamond detector has a diamond thickness of 30 micrometers. It has electrodes on the surface and is a test detector designed to determine the optimal electrode configuration for low ion energy. In the image, four distinguishable quadrants with their own numbering are visible. Each quadrant has a different electrode design, and the signal from ion detection can be retrieved from each quadrant individually. The first quadrant is called “Rounded” because of its unique curvature at the electrode edges. Although the second quadrant has the same electrode thickness as the first and third quadrants, it is called the "Thin" quadrant. The third quadrant is almost identical to the second, but equipped with an alloy plate on the back to connect the electronics to ground; this quadrant is referred to as "Thin Back." Lastly, the fourth quadrant has the largest electrode thickness; hence, it is called "Thick."

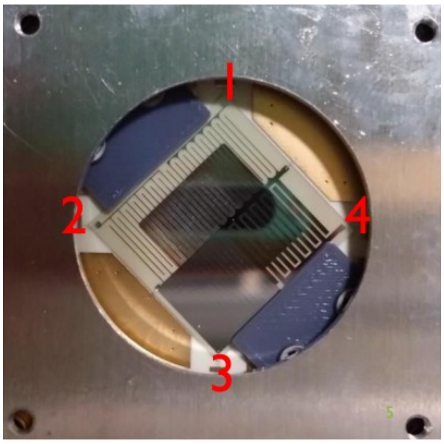

Figure 14: Image of test CVD diamond detector with labeled quadrants

This experiment is only a characterization of the diamond detector; therefore, a Radium-226 alpha source (Figure 15) with 4 kBq of radioactivity and a total energy of 4.78 MeV is used instead of TNSA-generated particles.

Figure 15: Radium 226 alpha source

To ensure the arrival of alpha particles at the detector, the detector is installed inside a vacuum chamber at a distance of 5 cm from the alpha source. An adjustable target holder is also installed in the vacuum chamber to reduce the ion energy during the low-ion-energy-efficiency measurement. A window is also located at the top of the vacuum chamber. Through the flange, cables connect the diamond detector to an oscilloscope for measurement. Between the detector and the oscilloscope, an amplifier is present. Two amplifiers were used separately to amplify the ion signal from the detector. The first detector is a shape amplifier, which shows the signal as a function of time, while the second is an integrated amplifier, which outputs the area under the signal curve. The experiment was initially performed with the integrated amplifier because the noise from the shape amplifier was too high. Later, once the noise was successfully removed, the shape amplifier was used to repeat the experiments for confirmation and to measure the response function. An image of the overall setup is shown in Figure 16.

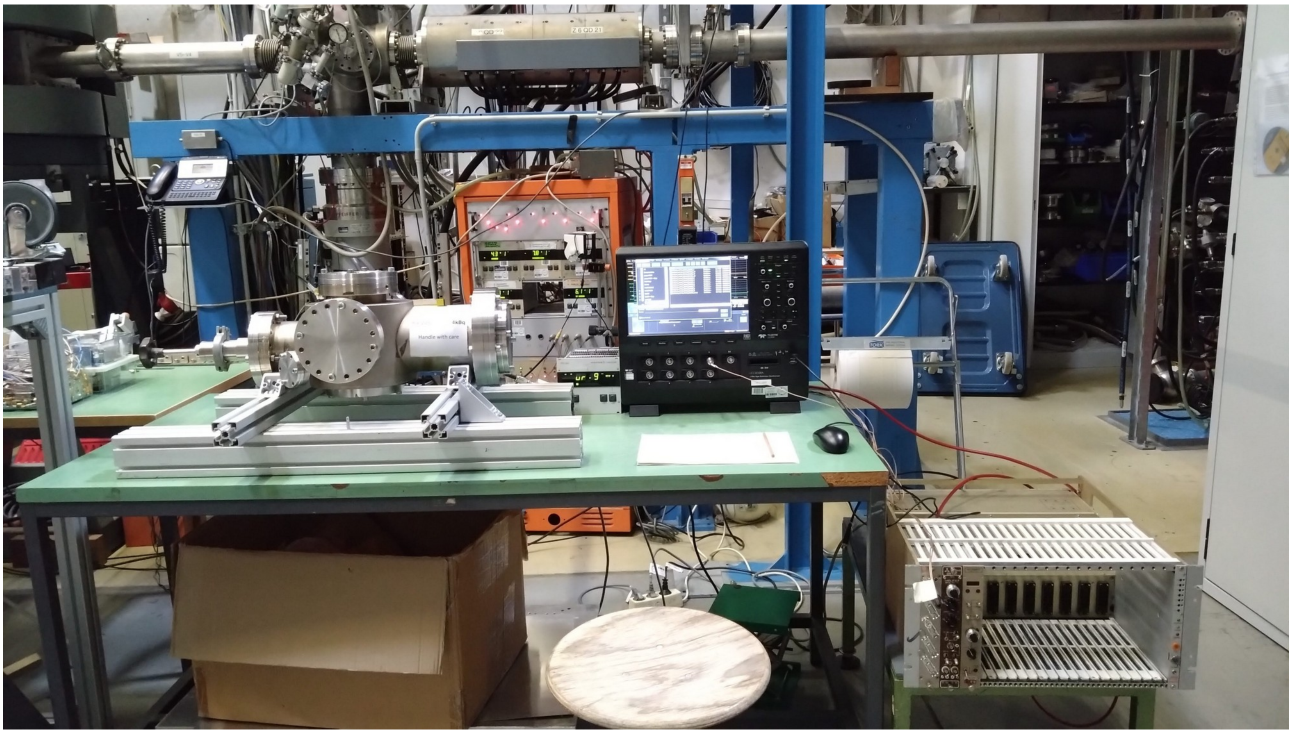

Figure 16: Setup of the experiment

With the setup established, the first experiment conducted was the bias-voltage efficiency experiment. The bias voltage is the potential difference between the electrodes; hence, a higher bias voltage results in a stronger electric field between them. Because the relationship between charge collection efficiency and input bias voltage is not affected by electrode design, this measurement was performed on only one quadrant of the detector. The measurement was performed by adjusting the bias voltage and averaging the peak signal at each value of the bias voltage. The mean peak signal is then plotted as a function of the input bias voltage.

The second measurement is the response function of each quadrant within the detector. The importance of the response function is to recover the actual characteristics of ions within experiments. The interaction between the ion projectile and diamond surface can be modeled as a delta function. However, due to the detector's internal electronics, the delta-function characteristics may not be directly observed. Nevertheless, the delta-function characteristics can be recovered by convolving the experimental data with the response function. This measurement is the simplest, as it only requires shooting the alpha source directly at the detector. The response function is simply the shape of the averaged signal obtained with the shape amplifier. Still, this measurement had the longest waiting time, as the average must be based on at least 1,000 measurements.

The last measurement is the charge-collection efficiency at low ion energy. In this experiment, the adjustable target holders are equipped with thin target foils of different materials to reduce the energy of the incoming projectile ion. A Python program was written to calculate the final energy of ions after traveling through any target foil or combination of 2 target foils available within the laboratory. In total, this experiment took significantly longer to complete, as measurements must be performed in each quadrant of the detector for each energy value. As the target holder can hold only up to four targets, considerable time was also spent changing the set of target foils and vacuuming the chamber after target replacements.

Result and data analysis

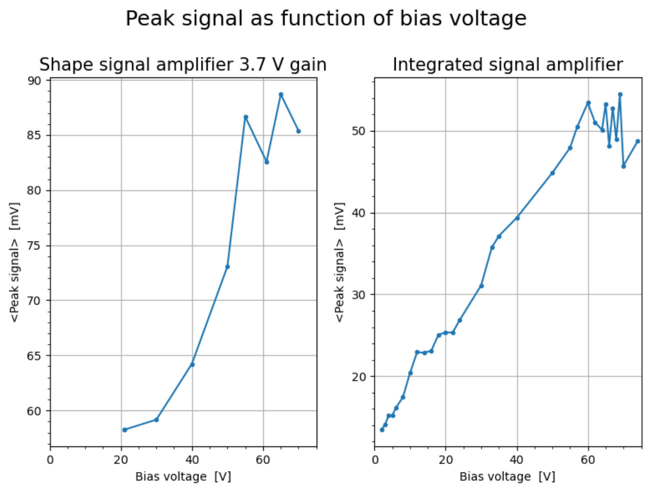

Figure 17: Plot of charge collection efficiency with respect to input bias voltage measured with both amplifiers

Plots of charge-collection efficiency with respect to input bias voltage from the integrated and shape amplifiers can be seen in Figure 17. Measurements from both amplifiers show agreement, with a positive correlation between the mean signal peak and the applied bias voltage observed up to 55 V. For this bias voltage, the mean signal peak oscillates around a constant baseline. The oscillation of the mean signal peak suggests that 55 V is the highest bias voltage that yields better separation and stronger drive of the electron-hole pair toward the electrodes. A higher bias voltage no longer yields a higher rate of electron-hole pairs separation; it only speeds up the rate at which electrons and their respective holes are driven toward the electrodes. Vice versa, bias voltage below

55 V is not strong enough to fully separate the electron-hole pair allowing recombination, resulting in a lower mean peak signal.

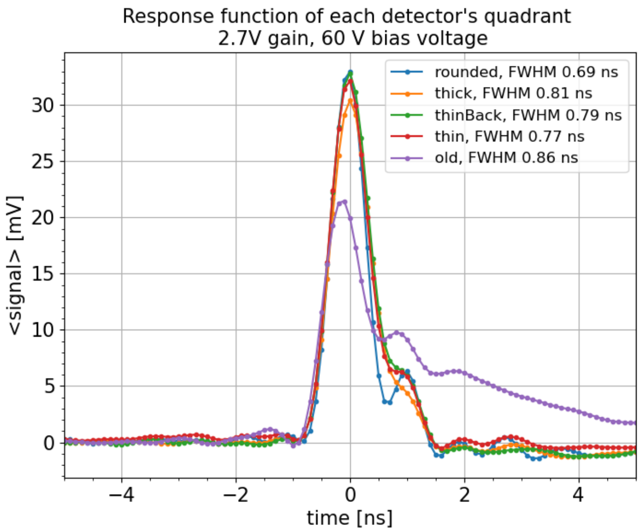

Figure 18: Plot of response function from each quadrants within the detector and older model detector

Recorded response functions for each quadrant within the detector, along with the older model with a sandwiched-electrode layout, are shown in Figure 18. In general, a better response function has a lower FWHM, as it better reflects the actual delta-function characteristics of the incoming ions. From the measurements, it is observed that the rounded quadrant has the smallest half-maximum; hence, it provides the best resolution in terms of the response function. By comparing the response functions across all quadrants, it is also observed that the newer design has better resolution than the older model, as indicated by a smaller FWHM.

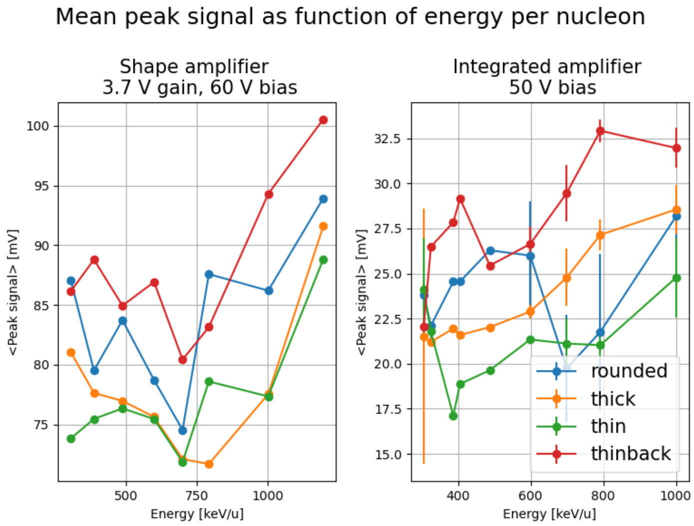

Figure 19: Plot of low ion energy measurement showing charge collection efficiency with respect to ion energy measured with both amplifiers

From the measurement of low-ion energy (Figure 19), Thin Back and Rounded quadrants show the highest charge-collection efficiency across all measured energy levels. The difference between Thin Back's high performance and Thin quadrant's poor performance suggests that the alloy plate connected to the Thin Back quadrant significantly increases charge-collection efficiency at low energy.

Combining the interpretations from each measurement, the best electrode design for low-energy ion detection is expected to be a new design of a Rounded quadrant with an allow plate in the back connected to ground or “Rounded Back”. This new design is expected to deliver the fast response time of the Rounded quadrant, combined with a high charge-collection efficiency, as the Rounded and Thin Back quadrants yielded the best charge-collection efficiency during the low-ion-energy measurement.

Suggestion for future improvement

During the section where the older diamond detector model was used, significant noise was observed. The noise is expected to be caused by the amplifier; therefore, a different type of amplifier, the DBA-II, is expected to help reduce noise during the experiment.

The second part of the improvement covers the data collection process. Currently, the data used to form the error bars for the low-ion-energy experiment were obtained by averaging multiple measurements of the mean. This process is suboptimal because it does not account for all the measurements. Therefore, an autosave function within the oscilloscope can be used to record each value, providing ag a better representation of the error bars.

References

[1] W. Cayzac *et al.*, “Experimental discrimination of ion stopping models near the Bragg peak in highly ionized matter,” *Nature Communications*, vol. 8, p. 15693, 2017, doi: 10.1038/ncomms15693.

[2] H. Nazary *et al.*, “Towards ion stopping power experiments with the laser-driven LIGHT beamline,” *Journal of Plasma Physics*, vol. 90, p. 905900302, 2024, doi: 10.1017/S0022377824000576.

[3] GSI Helmholtzzentrum für Schwerionenforschung GmbH, “PHELIX – Plasma physics with laser and ion beams.” [Online]. Available: https://www.gsi.de/en/work/research/appamml/plasma_physicsphelix/phelix

[4] GSI Helmholtzzentrum für Schwerionenforschung GmbH, “LIGHT – Laser Ion Generation, Handling and Transport beamline.” [Online]. Available: https://www.gsi.de/en/work/research/appamml/plasma_physicsphelix/experiments/light

4 Activities & Trips

So many memorable trips were made during our stay at the GSI summer school. There were so many activities that we wrote on the cover of our report book.

“OUR EXPERIENCE AT GSI-FAIR(-ENOUGH?): A QUANTUM SOUP MADE OF ALCOHOL, COFFEE, IONI CUDDLES AND TOURS WITH A SPRINKLE OF PHYSICS ON TOP.”

There were so many big and small trips we took that it would be impossible to document them all in this report within a finite number of pages. In case you wonder how many trips we have been to, here is a list of all folders of photos we have in our shared google drive: Archery, Basel Bad, BBQ, Big Tree, Bunny, Carbonara Day, Cocktail Night, Darmstadt, Darmstadt pedestrian rally, DnD, FAIR, Fanis Dinner, Fireworks Video, Frankenstein castle, Frankfurt 3/8 + 8/8/2025, Frankfurt museum festival, Freiburg, GSI, Heidelberg, Idstein, Ioni cup, Karaoke, Karaoke last day etc.

4.1 Plasma physics Waffle Wednesday

One special event, exclusive to the plasma physics faculty, is “Waffle Wednesday.” Every Wednesday at approximately 15 o’clock, every person working in the plasma physics department will gather at my shared office. In the image of my shared office (Figure 9), a waffle machine is visible. It is a fascinating tradition within the department because we not only cook waffles to eat together, but the person who cooks the waffles changes every week. Sometimes, the person cooking may bring their own secret ingredients, such as bananas or a crepe machine. It was an excellent time for people to come together and basically relax from work.

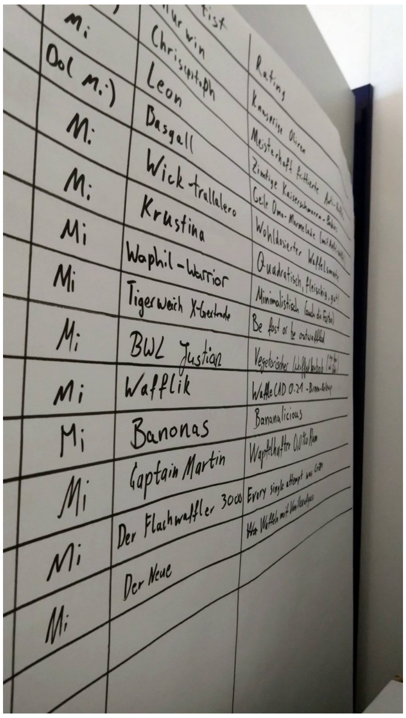

Figure 20: Rating sheet of plasma physics waffle Wednesday

Not only did we eat the waffles, but behind the office door is a big sheet of paper where we have to write down the chef, the week in the year, and the rating. As you might expect, all the details filled in here are completely unserious, from altering names (such as Jonas to Banonas) because he added bananas to his waffles, to a rating of Bananalicious. The mentioned rating sheet is shown in Figure 20.

4.2 Trip to Strasbourg

Figure 21: Photo taken infront of EU parliament in Strasbourg

Strasbourg is a city in France, near the border with Germany. At the first event, when most of the students were there, I was busy with work and did not join them. It may have been the right decision, as there were massive train delays, so they got back to the hotel at 3 am. Toward the end of my time at GSI, I decided it was time to go to some faraway places, and a small group was gathering to return to Strasbourg.

On this trip, there were four people in total. Initially, I was hesitant because of the small number of people and because I was not yet close to the others. Regardless, I went in and did not regret it. The four people were me, a guy who had no idea how long the trip would take, Debora, a small student from Italy, Felix (fun) from Germany, and Oier from the Basque Country, who always emphasized that his country is not part of Spain. As there were two Felixes in our program—one with enormous height and the other who goes out with us a lot—we decided to call them Tall Felix and Fun Felix, which explains the "(fun)" parentheses. Unknowingly, this trip turned out to be one of the most memorable of my life.

Our trip started early in the morning, around 5 or 6 am, if my memory does not play tricks on me. Catching the first train from a station next to the hotel, we hopped to the Darmstadt central train station and got some small bread for breakfast. As there were no direct trains to Strasbourg, we had to take about 4 train connections in total to get there. The path was through Heidelberg and many other breathtaking scenes. In total, the one-way path to Strasbourg takes approximately 4 hours by train.

As we arrived in Strasbourg, we went to get some food as lunch was approaching. I got a Kebab, which is a widespread food in Germany. We then walked around the city to the city's main cathedral, along a small river, and to the EU parliament. Although we didn't stay in Strasbourg for long due to time constraints, the trip was very fulfilling, as the best experiences were not the many beautiful places in Strasbourg but the strengthening of the friendships we made.

4.3 Frankenstein castle hiking trip

Not far from Darmstadt is a castle named Frankenstein, which may have inspired the famous novel. During this trip, Thanaporn and I had the chance to travel together with other students. With an unwavering heart toward hiking and zero sense of hiking direction, we set off on our trip to the castle.

Two of our friends left early as they wanted to bike there. Gladly, I did not join them as they got miserably lost and arrived almost an hour after us, who took a tram. I did not recall how long it took to reach that castle, but I do remember how our path became surprisingly confusing. We left the tram in what seemed like a small village. We then walked up a hill through a neighborhood. There, a hiking path leading to the castle was found. Some of my friends tried to look for natural walking sticks on the way, which they really enjoyed. From a clear hiking path, we somehow ended up on a small path—or no path at all—and basically followed the leader, who I am not sure really knew the way. The route got steeper and more natural (grass and leaves around our feet). Later on, we found ourselves on the main road leading to the castle, which was good if we had cars, which clearly we did not. That way, we started walking along the side of the road up to the castle.

As we arrived, we checked various areas of the castle, and our other friends who had ridden their bikes arrived some time later. We then went to a small restaurant in the castle, where we could chill and play cards. The hiking trip was surprisingly fun. On the way down, one of our friends even spotted a wild berry tree, which he collected for cooking at the hotel. I also tried the berry directly at the source; luckily, I am still alive.

Figure 22: Frankenstein hiking trip

4.4 Idstein trip

One of our friends heard from someone I don't know about a city we should visit during our stay in Darmstadt. From the brief we received, it was a small city in the north of Frankfurt that few tourists know about. It is a beautiful city with a structure that makes us feel like we are walking through a fairy tale. With this small information, our trip leader set up a trip to this mysterious place called Idstein.

The travel time to Idstein was relatively short, as it is located near Frankfurt. The stories about this city turned out to be true: it was really a small city with its charm as a clean, colorful city. We walked through the beautiful town, with buildings painted in shining, mesmerizing colors. There was a so-called "witch tower" in the town. There was a witch hunt or something similar in this city, and this tower, a few 10 meters tall, is a remnant of that event. We sat down in a cafe, played cards, visited a small church, walked past a shop showing antique toys from Star Wars, and so on. This small trip was really fulfilling for us all.

Figure 23: Group photo taken in Idstein

4.5 The big tree

This was a short, funny trip. One of our friends heard from her tutor that there is a big tree in a forest near GSI that we should go check out. The tutor said it so often that she decided to recruit about 10 people for this short trip. We rode our GSI bikes into a street next to GSI, which led us through a field and suddenly into a forest. Before entering the forest, we hesitated about whether we should really go into this dark forest. In the end, we decided to go in anyway. We rode our bikes following Google Maps directions through the forest and arrived at the main road, which Maps told us to cross. We gathered our courage, went all in, and decided to cross that highway.

On the other side of the road, there was a small, old, abandoned path. Again, we started to hesitate and jokingly say that this may be the plan from the tutor to murder us in a random forest with no escape. Still, we have come this far, so my 2 other friends and I decided to explore beyond the abandoned entrance of the road to see if there are further walkable paths. We discovered what seemed to be the path and called other people to join us, but we had to leave our bikes behind. Walking into that old, abandoned path, we continued deeper into the forest, where the path began to fade. There, an old bird-watching cabin was found, so two of our friends went up to scout, and we took some group pictures there. Then we started walking even deeper into the forest, without a clear path. Then, one of our friends saw a tree that looked different from the others, and there it was. The big tree that we all agree we have seen bigger.

Figure 24: The not so Big Tree

4.6 GSI Ioni cup

The Ioni Cup, a sports event, is organized annually at GSI. Everyone in GSI could form a team and participate. The sports in this event consist of running, archery, badminton, basketball, and volleyball. The summer students were split into about 3 or 4 teams. My team was called “4Fun”, and I was assigned as the team leader as my surname, Attapon, starts with the letter A. I played badminton with Meyhar, an Indian student studying in Michigan. The students have seen my badminton skills and really thought we were going to beat everyone else.

All the badminton matches were organized outdoors, which made wind and sunlight really difficult to deal with, but we had to make the best of it. We went against other summer student teams in the first and second matches. The first match was easy, but the second was a close win, as I was experiencing stage fright since this was my first actual badminton competition. The last match was the final game, in which we faced two GSI employees. This match was the most memorable badminton match in my life. As this was the final match, we agreed with the referee that we would play a standard international game with 3 sets. The competition was fierce. The opposition was the most vigorous opposition I have ever faced. Still, we managed to win the first set on a tiebreaker. In every set, the scores were so close that any minor mistakes could turn the game. We lost the second set. And the final set was upon us. We tried our best and fought competitively. In the end, we lost 21-19. Still, that was the most fun badminton match I've ever played.

Although we did not win in badminton, the GSI scoring combines all sports categories to determine the final ranking. As our teammate did really well in archery and basketball, we placed second and went home with a silver medal.

During my time at GSI, I've taken part in many more sports and enjoyed them a lot. I learned to play volleyball and now it is one of my favorite sports :)

4.7 Cooking Activities

On many of our free evenings, some of us gathered to cook together. Sometimes, it was a person cooking for everyone else. Sometimes, it was a small group of us cooking mojis. Sometimes, it was us all cooking panzerotis together.

Although I still don't remember the recipe for making moji, the others agreed that I was really good at making moji balls. They even called me the "Moji Machine." We mixed our own dough from scratch and heated it ourselves before putting in chocolate or marmalade. It was a fantastic bonding activity that tasted really good. On the second moji day, a friend of ours got some matcha, which gave our moji a fantastic taste.

After the hike from Frankenstein Castle, my friend who collected wild berries decided to cook pasta for everyone else. They all gathered to eat, but sadly I arrived too late and all the food was already gone. We always meet up in the hotel lobby during events. Somehow, that ordinary hotel became our space.

There was a night when we all decided to get together and make panzerotti, an Italian dish. If I were to explain it, then it is a fried dough filled with different fillings such as mixed pork, chocolate, or vegan. We were split into teams of filling and frying. I was in the filling team, and it was a lovely experience for me to cook this new recipe.

Oh, there was also a day that a small group of us gathered up to cook separately and share our food. My friend made a vegan tofu menu with incredible taste. On this day, I also had the opportunity to make some Thai-style omelets for them.

Figure 25: Self made Moji and Panzerotti

4.8 Food poisoning

The food we cooked together waswas fantastic, but ironically, I developed food poisoning during my stay at the hotel. This was an entirely avoidable mistake becausebecause I developed food poisoning from a piece of turkey that I kept in the refrigerator for too long.

With the unique opportunity to visit a German doctor, I carried myself there once I started to recover. Surprisingly, I did not have to pay for the doctor visit as the fees are charged directly to GSI. Hope this short message helps the next generation of GSI.

Appendix

Characterization of CVD Diamond Detector for Ion Stopping Power Experiments

Pititaras Attapon
Mahidol University International College, pititaras.att@student.mahidol.edu

A new design of a test diamond detector is characterized in terms of bias voltage efficiency, response function, and low ion energy efficiency to identify the most effective electrode design. Charge collection efficiency increases with applied bias voltage up to 55 V. By combining existing designs, the design of rounded electrodes with an alloy plate connected to ground is expected to provide the best performance in response time and low-energy charge collection.

1 Introduction

Ion stopping power refers to the energy loss per distance of an ion traveling through matter or plasma. It is essential to diverse experimental applications such as maintaining optimal self-heating of fuel pellets within Inertial Confinement Fusion reactors or studying kinematics of ions traversing through cosmic plasma. Although stopping power in plasma has been extensively studied, different theoretical models provide diverging predictions in the regime of low energy ion projectile where plasma's electron and the projectile's velocity are approximately equal. To improve upon the experiment performed with accelerator generated ions (as cited in [**?**]), a stopping power experiment at this low energy ions generated with lasers from LIGHT beamline collaboration is planned [**?**, **?**].

The "CVD diamond detector" is used to measure the ions' energy loss through Time of Flight (TOF) required to calculate the stopping power. In preparation for the stopping power experiment with the LIGHT beamline, this project aims to characterize the detector in three aspects, namely: 1. the efficiency with respect to applied bias voltage, 2. the response function of different detector designs required for recovery of incoming ion's signals without distortion from the detector's system, 3. the efficiency of different detector designs under low ion energy condition.

2 Experimental Setup

2.1 CVD Diamond Detector

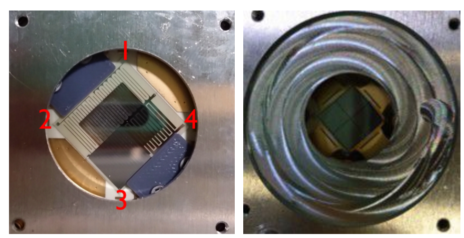

Fig. 1: *Image of the diamond detector with four distinct quadrants labeled as 1 to 4 (left) and the older model of sandwiched diamond detector (right)*

Ions traveling through the diamond within the detector ionize atoms within it creating electron hole pairs along the ion trajectory path. "Sandwiched" conducting electrodes placed on the top and bottom of the detector then separate the electrons and their respective holes to opposite sides, giving an electrical signal.

The diamond detector used in this report is a test detector with a diamond thickness of 30 μm. By placing both of the electrodes on the top surface to prevent electron-hole recombination in proximity, this detector is specifically designed for low ion energy. The detector contains four different rectangular quadrants with different electrode designs - shown in figure **??** along with an image of an older sandwiched detector design with a thickness of 13 μm. The first quadrant in the test detector is called "Rounded" due to its unique curvature on the electrode edges. Although the second quadrant has the same electrode thickness as the first and third quadrants, it is called the "Thin" quadrant. The third quadrant is almost identical to the second, but equipped with an alloy plate on the back to connect the electronics to ground; this quadrant is referred to as "Thin Back." Lastly, the fourth quadrant has the largest electrode thickness; hence, it is called "Thick".

2.2 Experimental Chamber

The experiments are conducted in a vacuum chamber including an alpha source, 4 kBq Radium 226 with a total energy of 4.78 MeV, aiming at the detector. A vacuum pump maintaining pressure of less than 10^{-3} mbar is connected to the chamber. In the low ion energy experiment, an adjustable target holder with thin foil targets is placed between the alpha source and the detector to reduce the energy of incoming ions to different levels. The alpha source and the detector are placed in close proximity to approximately 2 cm to ensure a sufficient counting rate at the detector.

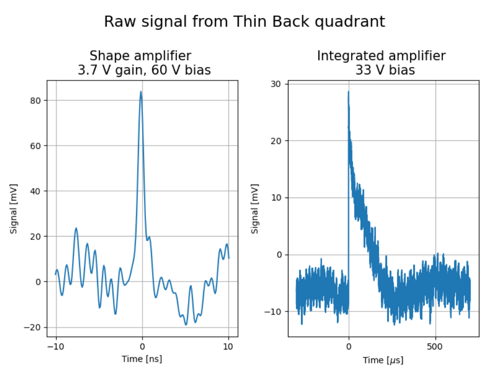

Fig. 2: *Example of raw signals from DBA-IV shape amplifier (left) and CSTA 2 integrated signal amplifier (right)*

The diamond detector is connected through the vacuum chamber to either a DBA-IV shape amplifier or a CSTA 2 integrated signal amplifier, both connected to an adjustable source of bias voltage applying a potential difference between the electrodes. If the shape amplifier is used, a gain voltage supply must also be connected. Finally, the amplifier is connected to an oscilloscope for the measurement. Figure **??** shows examples of raw signals recorded by the oscilloscope from the shape and integrated amplifier using the Thin Back quadrant. The peak in signal from the shape amplifier and sudden increase in the step function of the signal from the integrated amplifier correspond to an alpha particle.

3 Measurements

3.1 Bias Voltage Efficiency Measurement

To determine the detector's efficiency with respect to the applied voltage, the measurement is performed twice - first with the integrated amplifier, then with the shape amplifier with a gain of 3.7 V. The bias voltage connected to the amplifier is adjusted in steps, and the mean value of peak signals from alpha particles is recorded for each value of the bias voltage. As each quadrant shares the same characteristics in applied bias voltage, Thin Back quadrant is arbitrarily chosen for measurement.

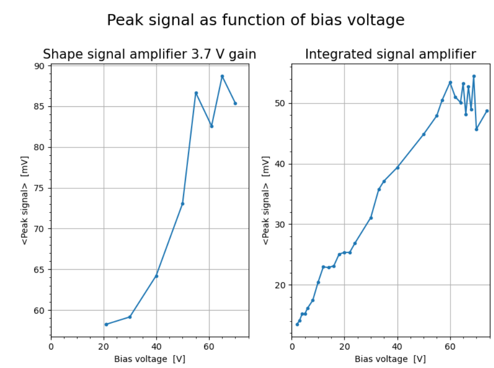

Fig. 3: *Plot of recorded mean peak signals with respect to bias voltage from shape (left) and integrated signal amplifier (right)*

Figure **??** shows the correlation between mean signal peak and bias voltage. Starting at 100 samples per bias voltage with the integrated amplifier, the number of samples is increased in steps of 100 throughout the measurement, being 300 at 14 V and 500 beyond 70 V. To confirm the result from the integrated amplifier, 1 000 samples are taken at each value of bias voltage when the shape amplifier is utilized.

3.2 Response Function Measurement

To recover the true signal of incoming ions, the convolution of the response function and the measured signal from experiments is required. Hence, a shape signal amplifier at a bias voltage of 60 V and 2.7 V gain is used to measure the response function of each detector design. By averaging 1 000 signals of alpha particles, the response function along with the “Full Width Half Maximum (FWHM)” of each quadrant in the test detector and the older detector model (figure ??) are shown in figure ??.

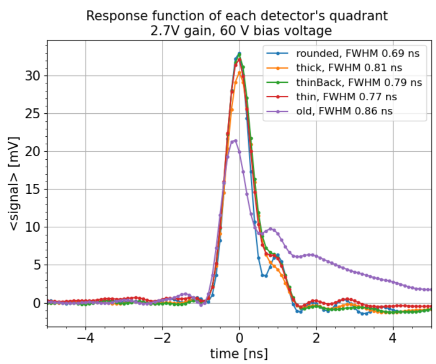

Fig. 4: *Measured response function of different diamond detector's quadrants and old detector model*

From figure ??, the asymmetric Gaussian shape of the response function is visible as the right tail of the function is longer than that of the other side. This property of the response function arises from the electronics of the detector, since it is common for the generated charge to be sucked away and generate a signal faster than the detector returns to its neutral initial state after signal detection.

3.3 Low Ion Energy Efficiency Measurement

The incoming energy of alpha particles is reduced by placing thin target foils between the alpha source and the detector to characterize the detector's performance at lower ion energy. With simulation software such as SRIM and knowledge of “ion cold-matter interaction” [?], the energy loss of alpha particles passing through target foils can be calculated. Combinations of different thin target foils reducing the ion energy to a preferred level are determined and inserted into the vacuum chamber.

By averaging three to four hundred samples at each energy level using the integrated amplifier at a 50 V bias voltage and the shape amplifier at a 3.7 V gain and 60 V bias voltage, the average peak signal at different energies of ions arriving at the detector for all quadrants of the

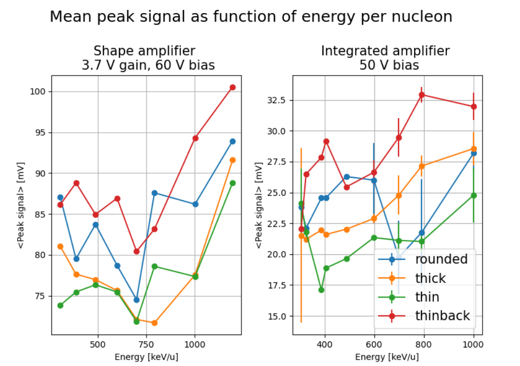

Fig. 5: *Mean peak signal as function of ion energy per nucleon for shape (left) and integrated (right) amplifier*

test detector is measured (figure ??). In this figure, only some data points from the integrated amplifier contain error bars. Initially, the error bars are calculated from the mean value of three separate measurements of 100 averaged signals. However, this setting does not provide enough statistics for analysis; the setting is later altered to use all the signals consecutively to increase the number of samples at the cost of lacking error bars.

4 Results & Discussion

Regarding the charge collection efficiency with respect to the bias voltage (figure ??), at 1 Volt bias voltage with the integrated amplifier, the detector is able to record a signal from the alpha particles, showing its capability at low bias voltage. However, for the shape amplifier, signals from bias voltages less than 21 Volts are not observed due to higher noise levels. The peak signals of both amplifiers are correlated positively with increases in bias voltage up to about 55 V. The signals' peak then oscillates around a constant value at higher bias voltages. This result suggests that increasing bias voltage beyond 55 V does not correlate to higher efficiency of charge collection. The reason for the oscillation around a constant baseline is currently inconclusive, but it is unlikely to be caused by data size as the result from the shape amplifier with a higher number of data points shows the same characteristics.

From the measurement of the response function in figure ??, each electrode design shows approximately the same start of rise time at about −1 nanosecond, specifying an indifference in the initial response time for each design. A smaller FWHM of the response function corresponds to higher detector resolution as it better reflects the characteristic delta function shaped signal of ions. From the figure, the Rounded quadrant has the smallest FWHM, indicating it has the best resolution. Furthermore, comparing the response functions from each quadrant with those of the older model, each quadrant shows a higher peak value and a smaller FWHM, specifying an improvement in charge collection efficiency and response time from the older model.

From figure **??**, the Thin Back and Rounded quadrants outperform the other two quadrants in terms of charge collection efficiency at every measured ions' energy level, as they always provide higher peak values. Thin Back's outstanding performance and the Thin's poor performance suggest that the alloy plate inserted into the Thin Back quadrant significantly improves the performance. The result from the integrated amplifier shows a positive correlation between mean peak signal and energy per nucleon throughout; however, the result from the shape amplifier shows a trend similar to a local minimum at approximately 680 keV/u. What appears to be a local minimum could be a constant line. One possibility for the distinction between trends from the two amplifiers is that the shape of the signal at lower energy may have a lower peak but a wider FWHM, contributing to a constant increase in integrated area when measured with the integrated amplifier.

From the three aspects of characterization of the CVD diamond detector, the Rounded and Thin Back quadrants perform outstandingly in terms of response time and charge collection at low ion energy. Combining the two designs, a new design with rounded corners and an alloy plate on the back side connected to ground ("Rounded Back") may significantly contribute to higher efficiency.

Significant improvements are possible in two areas. The first one is a reduction in the high noise level of up to 20 mV, caused by the DBA-IV shape amplifier. Noise may be reduced by replacing it with a DBA-II amplifier, which is known for better noise control allowing detection of weaker signals from the shape amplifier. Second, using the oscilloscope's auto-save function to record individual signals would allow for error bar calculation, greatly improving the analysis of mean values and local minima in low-energy measurements.

5 Conclusion

With an alpha source and a vacuum chamber, the test CVD diamond detector's bias voltage efficiency, response function, and low ion energy efficiency were characterized using both shape and integrated amplifiers.

Up to a bias voltage of 55 V, the peak signal increases with the input bias voltage. However, at higher bias voltages, the signal does not rise further, but oscillates around a constant baseline. This indicates that increasing the bias voltage beyond 55 V does not enhance the signal output.

Combining the fast response time and high charge collection efficiency of the Rounded and Thin Back quadrants, a combination of the design features of the two has the potential to improve the detection efficiency of the diamond detector.

By replacing the DBA-IV shape amplifier with the DBA-II model to reduce noise from the shape amplifier and recording each single signal contributing to the mean for error bars, the detection of low signal output can be improved and the local minima trend obtained from the shape amplifier in low ion energy measurements can be better analyzed.

Acknowledgment

I would like to express my gratitude to the plasma physics group at GSI, especially Abel Blazevic, Denis Schumacher, Marvin Fischer, and Kristina Lerner for their significant contributions and support in this project.

To the summer students: "The world is a village—we always meet again." − Random DB driver P.S. In Mus, two kings are low.

References

[1] H. Nazary, "Towards ion stopping power experiments with the laser-driven LIGHT beamline," PhD thesis, Technische Universität Darmstadt, July. 2024.

[2] K. Lerner, *Stopping Power Experiments with the Laser-Driven LIGHT Beamline*, Master thesis proposal, Technische Universität Darmstadt, Jun. 2025.